Journal of
MATERIALS RESEARCH

Electronic states in heavily Li-doped graphite nanoclusters

M. Yagi, R. Saito, and T. Kimura
Department of Electronics Engineering, University of Electro-Communications, Chofu, 182-8585 Tokyo, Japan

G. Dresselhaus
Francis Bitter Magnet Laboratory, Massachusetts Institute of Technology, Cambridge, Massachusetts 02139

M.S. Dresselhaus
Department of Electrical Engineering and Computer Science and Department of Physics, Massachusetts Institute of Technology, Cambridge, Massachusetts 02139

(Received 22 February 1999; accepted 25 May 1999)

Negative ion states for Li atoms are found in graphite nanoclusters heavily doped with lithium using a semiempirical calculational method. These calculations identify a quasi-stable site for a negative Li ion near the terminated hydrogen atoms, and this site becomes very stable in the presence of the Coulomb interaction between Li ions. The total charge transfer from Li ions to the graphite clusters does not depend on the number of Li atoms per cluster but rather on the relative geometries of the Li atoms on the cluster. The relationship of these findings to the findings in the ^{7}Li nuclear magnetic resonance experiments and to the performance of Li secondary batteries is discussed.

I. INTRODUCTION

Recently noncrystalline graphite clusters with diameters in the nanometer range have attracted worldwide interest with regard to high-performance secondary batteries, especially for electric vehicles. When graphite host materials are prepared as a negative electrode using pyrolytically treated hydrocarbons, the charge and discharge performance of the battery increases up to 700 mA h/g, which is much larger than the 372 mA h/g which is obtained for first-stage Li graphite intercalation compounds (GICs), LiC_6, and other materials.[1–7] In the nanocluster case, Li ions can be absorbed on the nanoclusters up to a stoichiometry of LiC_2, which has three times as many Li atoms at LiC_6.[1] Such a high Li density cannot be obtained in GICs, except for the high-density phases of GICs under pressure, such as LiC_3 and LiC_2.[8–10] It is thus important to explain why more Li atoms can be absorbed on small graphite clusters at ambient pressures than in a stage 1 GIC.

Nanographite clusters, consisting of several layers of graphitic planes with a small area, are obtained by the heat treatment of various pregraphitic carbons, such as polyparaphenylene (PPP)[1,2] and pheno–formaldehyde (polyacenic semiconductors, PAS),[3,11,12] at temperatures from 700 to 900 °C, where the hydrogen atoms of the precursor hydrocarbon molecules are dissociated from the carbon atoms,[13] and the nanographite is formed by connecting the dangling bonds of the carbon atoms thus generated. Another type of nanographite cluster stems from porous carbon structures, such as activated carbon fibers (ACFs) and carbon aerogels, whose specific surface areas can be as large as 3000 m^2/g.[14] Here the large surface area or the many edge sites of the cluster play a key role in achieving high Li concentrations. Since the charge–discharge performance of a Li ion battery depends on the size of the nanographite,[13] the threefold enhancement in the Li uptake relative to that for the stable LiC_6 GIC comes from finite size effects associated with the nanographite cluster. Furthermore, according to the ^{7}Li nuclear magnetic resonance (NMR) spectra, there are two possible Li states:[1,4,6,7] one is an ionic state, and the other is a molecular state for the Li atoms. Thus an electronic structure calculation of a Li-doped graphite cluster is important for investigating the origin of stable Li sites on a graphite cluster.[5]

At the edge of a nanographite cluster, hydrogen atom terminations of the carbon atoms or of the dangling bonds are expected from experimental considerations.[5] When Li atoms make a strong covalent bond with the dangling bond from the carbon atom, the Li absorption process becomes irreversible in secondary batteries, which may be consistent with the irreversible portion of the discharge curve that is observed in secondary batteries.[3,12] This irreversible portion of the discharge/charge

curves can also be understood by the oxidation of the surface, which is known as the solid–electrolyte interface (SEI).[15,16]

As for the hydrogen-terminated edges, Nakada *et al.* showed that there are special electronic states of the valence π electrons at the Fermi energy and that these special states are localized at the so-called zigzag edges of a nanographite cluster.[17] Since there are no states at the Fermi level in the case of armchair edges, the number of edge states in the nanographite cluster is dependent on the shape of the edge. The edge state which is partially occupied by electrons at the Fermi level plays an important role in accepting electrons. In fact, we calculated the electronic structure of a Li ion at the edge of a hydrogen-terminated nanographite in a previous report[18] (see also Ref. 5) and found that the Li ion has an ionicity of $+0.6e$ at the hydrogen-terminated edge and that the donated electron to the nanographite cluster is distributed over the edge carbon sites.[18] Furthermore, Li–Li bonding on a finite-size cluster can even give negative ionicity by occupying the molecular orbitals corresponding to Li 2*s* orbitals.[18] However, in the previous paper we did not put as many Li ions on the cluster as is possible. Thus, the subject of the present paper is the uptake capacity and the stability of Li atoms on a nanographite cluster.

In this paper we calculate the electronic structures of Li-doped nanographite for many stable positions of Li atoms and for a variety of relative positions so as to reproduce the experimental geometry. We previously found[18] that the total charge transferred to the graphite cluster has large variations in value for different Li configurations, and these differences in the charge transfer associated with the interior and edge sites give rise to the two peaks that are observed in the ^{7}Li NMR experiment.[1,4,6,7] In Sec. II, we briefly explain the calculational method and the geometry of the nanographite cluster that we used in the present calculation. In Sec. III, the calculated results are presented for a Li-doped nanographite cluster. Finally, a summary of our results is given.

II. METHOD

For our calculations we adopted a hexagonal $C_{54}H_{18}$ cluster in which 18 carbon (C) atoms are terminated by hydrogen atoms at the edge, and the other 36 C atoms are located in the interior region of the cluster, as shown in Fig. 1. We also calculate the electronic structures of Li ions on hexagonal $C_{24}H_{12}$ and $C_{96}H_{24}$ clusters, from which we can obtain insight into the dependence of the lithium uptake on the nanocluster size. The $C_{24}H_{12}$ cluster seems to be too small to gain an understanding of the possible stable Li edge sites, and the $C_{96}H_{24}$ cluster is large regarding the amount of computational time that is necessary for considering many Li atoms in different

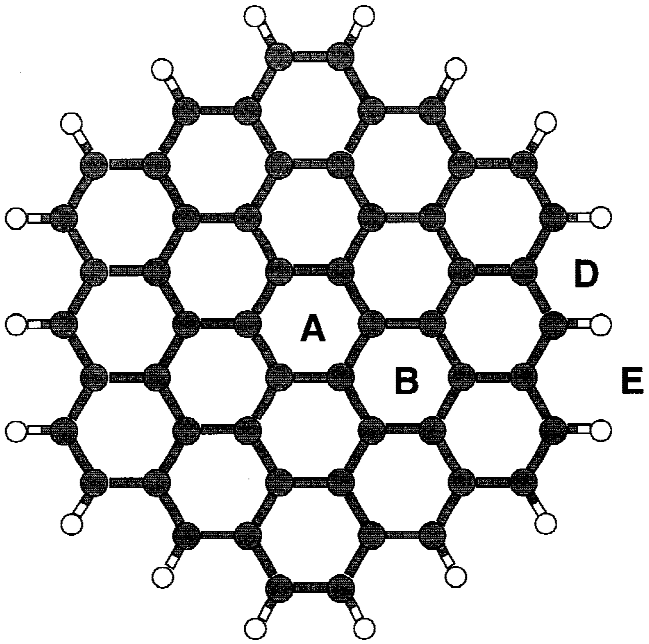

FIG. 1. $C_{54}H_{18}$ cluster. A or B are interior stable Li sites between which there is a local maximum with the energy barrier of 0.12 eV. D or E are edge sites whose ionicities are positive and negative, respectively. Although the finite size effect may affect the above value, the above statements do not depend on the cluster size, at least up to the $C_{96}H_{24}$ cluster.

geometries. The cluster size of $C_{54}H_{18}$ is, however, suitable for the present investigation, and the essential physics for nanographite clusters can be reproduced in this cluster size, as shown below.

In the calculations, we put Li atoms, one by one, on a cluster and the initial positions of the Li atoms are above or below the nanographite cluster (i) at the center of the hexagonal carbon ring, or (ii) at an edge site surrounded by three carbon atoms and by the two hydrogen atoms, which terminate the dangling bonds on the carbon atoms, as shown in Fig. 1. These sites are known as stable sites for a Li atoms on a nanographite cluster,[18] and in fact, the optimized Li sites are one of these stable sites. The bond lengths and bond angles are optimized by using the semiempirical quantum chemistry library, MOPAC93, in which the parametric method 3 (PM3) for an interatomic potential is adopted in the present calculation.[19] We also checked some geometries by *ab initio* calculations to obtain the same optimized geometry and ionicity within the accuracy discussed in this paper.

The electronic structure calculation for valence electrons is simultaneously given within the unrestricted Hartree–Fock (UHF) method for an odd number of electrons in the MOPAC93 library. It is known that the bond length and the heat of formation energy obtained by the PM3 potential reproduces these quantities for many known molecules very well, since the parameters of the PM3 potential are obtained so as to minimize the stan-

dard deviation of the physical properties for many molecules on the basis of experimental values.[19] The semiempirical method is suitable for calculating the electronic structure of the cluster for many different configurations of Li sites, so as to get a clear view of the physics that is involved.

III. CALCULATED RESULTS

For a $C_{54}H_{18}$ cluster, we can put up to 24 Li atoms on the nanographite cluster. When we put additional Li atoms on the nanographite cluster, the Li atoms apparently form Li metallic clusters, which seem to be independent of the graphite cluster, and such metallic clusters are therefore excluded in the following discussion.

As we found in a previous paper[18] the edge region of the graphite nanocluster is more stable by several electrovolts for Li atoms than is the interior region. Thus, even when we put Li ions in the internal region of the cluster as the initial positions for these ions, we often find that the optimized Li positions are in the edge region, unless the number of Li ions is sufficiently large to fill the edge sites. This placement of the Li ions occurs because the energy required for sliding the Li atoms on the graphene plane is small compared with the gradient of the potential that is used in the optimization process of the calculation. In fact, when we calculate the adiabatic energy of the cluster as a function of fixed Li positions from the center A of the central hexagon to the nearest neighbor center B in the $C_{54}H_{18}$ cluster, as shown in Fig. 1, we have a local maximum of 0.12 eV in the middle of the adiabatic path. Since this energy barrier is on the order of the energy of optical phonons, we expect Li ions to move freely on the surface of the interior region when the energy fluctuations due to molecular vibrations or other interactions take place. This result is consistent with the temperature dependence of ^{7}Li NMR experiments[4,7] in which the Li ions are diffusive at the room temperature. When we put several Li ions in the interior region as an initial position for the lattice optimization, the Li ions are pushed out to the edge sites by their Coulomb repulsion. In contrast, when we carry out a similar calculation for an F atom, energy barriers of 1.8 eV are obtained, so that the F atoms cannot move on the nanographite cluster once the F atom becomes bonded to carbon atoms.[20]

In Fig. 2 we plot the total charge transfer of electrons from Li atoms to the nanographite cluster in units of *e* as a function of the number of Li ions, *N*. Here a positive value of the total charge transfer in Fig. 2 corresponds to a net electron donation to the graphite cluster. Each open circle and each cross denote the result for a cluster where Li ions are located over the cluster and only at the edge sites, respectively. Even for the same *N*, the total charge transfer values depend strongly on the clusters in which

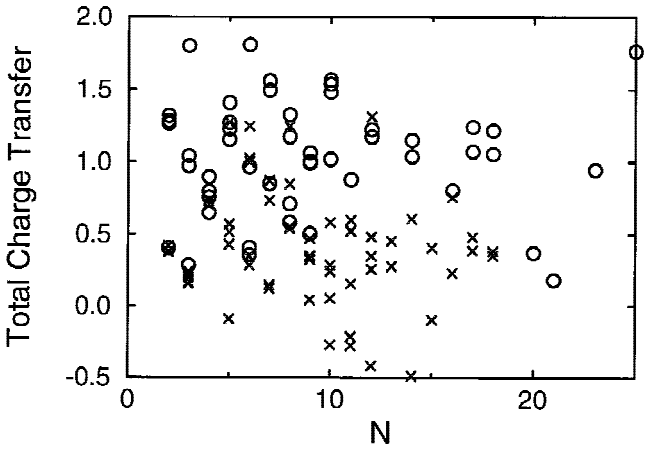

FIG. 2. Total charge transfer of electrons in units of *e* as a function of Li number *N* for $C_{54}H_{18}Li_N$ clusters. Open circles and crosses, respectively, denote the geometries in which Li ions are distributed over the interior of the cluster or are only at the edge region.

the geometries of the Li ions are different from each other. When *N* is very small, the total charge transfer increases with increasing *N*. However the total charge on the cluster quickly saturates for small numbers of Li atoms, compared with the saturated number of Li atoms. Here the saturated number is defined by the maximum number of Li atoms which can be adsorbed without forming a Li metallic cluster. In the cases of $C_{24}H_{12}$ and $C_{54}H_{18}$, the saturated numbers of Li atoms are 14 and 24, respectively. These numbers correspond to the Li atoms with the $\sqrt{3} \times \sqrt{3}$ structure of C_6Li at the two sides of the graphitic plane and to Li atoms at edge sites surrounded by hydrogen atoms.

When a Li ion is isolated on a cluster and free from interactions with other Li ions, the ionicity of the Li ions is $+0.6e$. However, the calculated ionicity of Li ions in the cluster consists of two groups: One is around $+0.6e$ as for the isolated Li ion, and the other is negative around $-0.3e$. Especially the negative ions in the interior region and in the edge region have an ionicity from $-0.4e$ to $-0.3e$ and from $-0.4e$ to $-0.2e$, respectively. Because of the different sign of these ionicities, the fluctuation of the total charge increases with increasing *N*, depending on the relative positions of each added Li ion.

In Fig. 3 we show the top and side views of a $C_{54}H_{18}Li_{14}$ cluster in which the charge of the Li ions are labeled. In this cluster, we found that some optimized Li ion positions are located in the interior region. This optimized geometry is suitable for explaining the reason for the occurrence of the negative Li ions, as is discussed below. In this cluster we found six negative and eight positive Li ions, as shown in Fig. 3. In the center of the cluster we found two Li ions above and below the center of the hexagon whose charges are $0.63e$ and $-0.33e$, respectively. A similar situation of two Li ions is observed in the left-top region, but in this case, both the Li

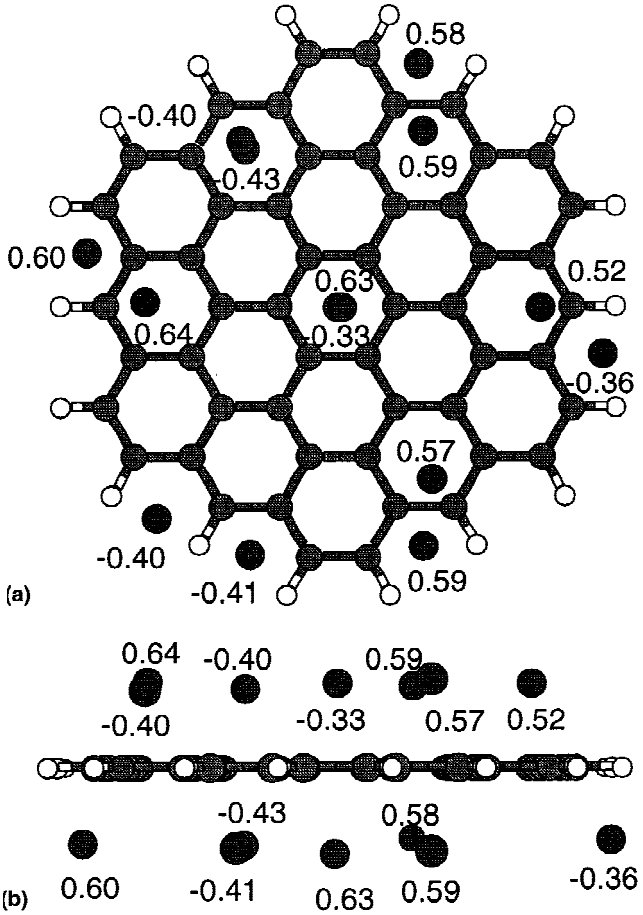

FIG. 3. (a) Top and (b) side views of a $C_{54}H_{18}Li_{14}$ cluster in which the charge of each Li ion is labeled. In this cluster we found six negative and eight positive Li ions. We did not find any situation in the $C_{54}H_{18}Li_N$ clusters where two Li ions are on nearest-neighbor sites at the centers of the hexagons and on the same side of the graphene layer.

ions have negative charges, $-0.40e$ and $-0.43e$. In the edge region, three negative ions whose charge is around $-0.4e$ are found and the other Li edge sites have $0.6e$ positive ions. We can find pairs of positive Li ions near the edge region for which the Li ions are on different sides of the graphene layer from each other. Although the cluster in Fig. 3 is not a typical result among the many optimized geometries, this cluster is selected for illustrative purposes because it shows a variety of interesting situations in a single cluster. It is noted here that we did not find the situation in any cluster that two Li ions are stabilized in nearest-neighbor hexagonal centers on the same side of the graphene layer, which is consistent with the other theoretical work by Zhou *et al.*[5]

When we investigated the ionicity of the negative Li ions, we found two possible origins for this phenomenon. One occurs for the Li ions in the interior regions, and the other occurs for the edge Li ions. The origin for the stability of the interior Li ions is the overlap of the Li wave functions. Since there is an interaction between the 2*s* orbitals of two nearby Li atoms, the molecular states associated with the Li 2*s* orbitals split into molecular orbitals with different energies. When a Li atom has many components of the occupied molecular orbitals, the Li atom can have a negative ionicity. This does not happen in the case of the electronic structure of the periodic Li lattice in which the self-consistent charges of the Li atoms are all equal because of symmetry. The negative Li ionicity is thus a kind of finite size effect which arises from symmetry breaking, so as to minimize the total energy. When we only consider this origin for the negative ionicity of the Li ions, the negative Li ions would tend to disappear on a nanographite surface with large *N*. The fluctuations in the total charge transfer due to this process quickly decreases with increasing numbers of Li ions if the Li atoms are packed in the interior region. When Li atoms are distributed inhomogeneously, fluctuations in the Li ionicity can be expected, depending on the size of the isolated Li clusters on the nanographite.

Another origin of the negative charge of Li ions is their location at special stable sites for Li ions around the hydrogen terminated carbon edges (see Fig. 1). When we investigated the optimized positions of Li atoms at the edge, the self-consistent charge distribution depends strongly on the position of the Li site. In Fig. 4(a) we plot the optimized "height" of the Li atoms from the graphitic plane as a function of the distance from the center of the cluster. In the interior region, since the stable Li sites are above the center of the hexagonal ring, the position of the sites from the center appears at several discrete positions. However, around the edge, the positions of the stable Li sites are distributed continuously, reflecting the shape of the cluster and the many possible edge sites. An interesting feature of Fig. 4(a) is that the stable Li height changes quickly around the hydrogen terminated position. In Fig. 4(b) we plot the self-consistent charge as a function of the Li height. It is clear that the charge becomes negative for values of the height smaller than 1.8Å. A typical example of a negative Li ion in the edge is the $C_{54}H_{18}Li_2$ cluster in which only two Li ions are located on the opposite edges and on the opposite side of the graphitic plane from each other. In this case the ionicities of the Li ions are $0.60e$ and $-0.22e$, respectively. This situation cannot be explained by the overlap of Li 2*s* orbitals.

When we considered a plane intersecting two hydrogen atoms and perpendicular to a graphitic plane, we found that there are two stable sites for Li ions: One is on the graphite side (D in Fig. 1), the other is on the outer side of the plane (E in Fig. 1), and these two sites have positive and negative charges, respectively. The negative charge states tend to appear preferentially at stable sites near the outer side, where the Li forms a small cluster with two hydrogen atoms,[5] in which typical ionicities of the Li and H are $-0.26e$ and $0.14e$, respectively.

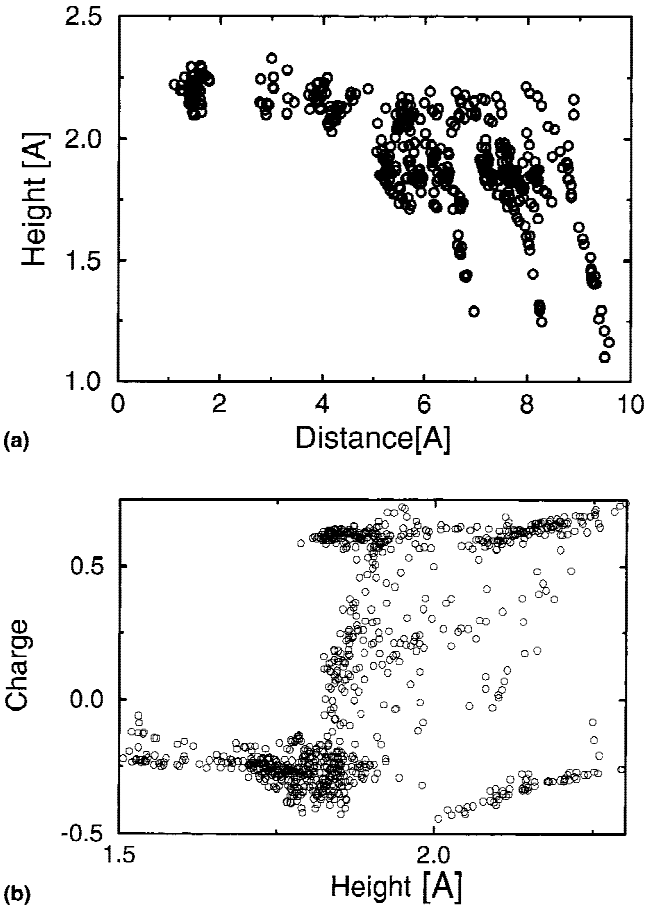

FIG. 4. (a) The optimized heights of Li ions from the graphitic plane as a function of the distance from the cluster center. (b) Li ionicity as a function of Li height. The Li heights in (a) and (b) are the same. Points are takes for Li ions in $C_{54}H_{18}Li_N$ for each N value, using many different geometries in order to approximate the real system.

The negatively charged Li sites are energetically unstable compared with the positively charged Li sites. Thus if there is only a single Li atom on the cluster, we will always get a positive Li ion, which is consistent with the results presented in the previous paper.[18] In the case of two Li ions which are both stabilized at the edge, one of them is a positive ion and the other is a negative ion. The reason we find one of the two ions to be a negative ion is due to the interactions between Li ions. If the two Li ions are positive ions, the repulsion between the Li ions pushes the Li ions out from position D near the carbon atoms to position E near the hydrogen atoms (see Fig. 1), and this shifted position makes the Li ions negatively charged. Since the absolute value of the negative charge is not as large as the value of the positive ion, the interaction between the negative and positive charges is not so large as to push the Li ion back to the stable site. It is pointed out here that when two Li ions are in the interior region, the Li ions are both positive ions in most cases, because there are no quasi-stable sites at which Li ions become negative ions.

It should be mentioned that the first origin of the negative ions, the Li 2*s* overlap effect, can occur for Li ions in the edge regions when there are neighboring Li ions in the edge or interior regions. In that case the Li ions at the position D in Fig. 1 can be negative ions, which can be seen in Fig. 3. It is clear from Fig. 4 that all Li ions at the position E in Fig. 1 are always negative.

The reason why we get negative Li ions is that there are stable sites made by two hydrogen atoms.[5,18] In fact, if we calculate the energies for a LiH_2 clusters, the Li ions become negatively charged at an ionicity of $-0.14e$. However, if the geometry of the LiH_2 molecule is optimized by fixing the H–H bond length to the value in the $C_{54}H_{18}$ cluster, the Li ions have an ionicity of $+0.16e$. If the hydrogen atoms are close enough to each other, the bonding molecular orbitals, consisting of hydrogen 1*s* and Li 2*s* orbitals, become sufficiently lower in energy, so that they can accept an additional electron from the H 1*s* orbitals to the Li 2*s* orbital. This is the reason why isolated LiH_2 clusters form. In the nanographite system, the situation becomes complicated since the bonding molecular orbitals are coupled with delocalized carbon orbitals. Even in that case, calculations of the components of the Li 2*s* orbitals in the molecular orbitals are essential for determining the ionicity of the Li ions.

For small N, all the Li ions can be positive ions for a geometry where the Li ions are apart from each other and are in the interior region. When N increases, the number of negative ions increases, and thus the total charge transfer becomes saturated in the middle density range of the Li ions. The ratio of the number of Li negative ions to N for the $C_{54}H_{18}Li_N$ cluster becomes 0.5 when N becomes relatively large. (For example, $15 \leq N \leq 24$ for the $C_{54}H_{18}Li_N$ cluster. The maximum number of Li ions is 24 for the $C_{54}H_{18}Li_N$ cluster.) For larger values of N, the total charge transfer thus becomes positive as shown in Fig. 2. The stable Li sites found in this paper are the sites which give rise to the two peaks in the ^{7}Li NMR experiment. These calculations are consistent with the experimental observation that the Gaussian NMR peak corresponding to the negative ions is broader, indicative of the larger variation of the ionicity for the negative Li ions, which support an inhomogeneously broadened NMR line.[1,4,6,7] The intensities of the two NMR peaks as a function of the cluster size and of the Li concentration[6] would provide a good indicator for specifying the charge of the Li ionic states.

In order to improve the performance of Li ion batteries, the number of negative ions should be decreased. When we consider the effect of hydrogen and the Li 2*s* overlap effect that are possible origins of the negative ions, only the Li 2*s* overlap effect may be modified by changing the electronic structure of the π electrons of nanographite. The one electron energies of the Li 2*s* molecular orbitals depend on the delocalized π orbitals of

the nanographite. Even though the two Li ions on the cluster are separated from each other, the two Li 2*s* orbitals can interact via the Li–C interaction. If the carbon π orbitals are sufficiently localized compared with the size of the cluster or the Li–Li distance, the indirect Li–Li interaction and the fluctuation of the one-electron energies of the Li 2*s* molecular orbitals might be reduced. This is the opposite limit of the finite size effect of the graphite crystal. In the atomic limit of carbon, it is clear that the fluctuation of the Li ionicity in a C–Li cluster disappears. In this case the charge transfer of an electron from Li to C occurs because of the difference of the one-electron energies between the Li 2*s* and C $2p_z$ levels. This can be a reason that a small amount of boron substitution for the carbon atoms affects the improvement of the performance of the battery significantly.[5] Additional calculations or experiments are necessary to investigate this problem further, and such work will be reported in the future.

IV. SUMMARY

In conclusion, we have calculated the electronic structure for Li-doped nanographite clusters. In particular, the negatively charged states of the Li ions are investigated in the cluster calculation with different geometries for the Li ions. The origin of the negative ions comes from the finite size effects of the cluster, which are important both in the interior and in the edge regions of the cluster.

ACKNOWLEDGMENTS

The authors thank Prof. T. Enoki, Prof. H. Tohara, and Prof. M. Endo for stimulating discussions and for sharing their experimental data prior to publication. Part of the work by R.S. was supported by a Grant-in Aid for Scientific Research (No. 10137216 and No. 09243105) from the Ministry of Education and Science of Japan. The MIT work was partly supported by the National Science Foundation (Grant No. DMR 98-04734).

REFERENCES

1. K. Sato, M. Noguchi, A. Demachi, N. Oki, and M. Endo, Science **264,** 556 (1994).
2. M. Endo, K. Takeuchi, S. Igarashi, K. Kobori, M. Shiraishi, and H.W. Kroto, J. Phys. Chem. Solids **54,** 1841 (1994).
3. S. Yata, Y. Hato, H. Kinoshita, N. Ando, A. Anekawa, T. Hashimoto, M. Yamaguchi, K. Tanaka, and T. Yamabe, Synth. Met. **73,** 273 (1995).
4. K. Tatsumi, J. Cornard, M. Nakahara, S. Menu, P. Lauginie, Y. Sawada, and Z. Ogumi, Chem. Commun. 687 (1997).
5. P. Zhou, P. Papanek, C. Bindra, R. Lee, and J.E. Fischer, J. Power Sources **68,** 296 (1997).
6. S. Yamazaki, T. Hashimoto, T. Iriyama, Y. Mori, H. Shiroki, and N. Tamura, J. Mol. Struct. **441,** 165 (1998).
7. S. Wang, H. Matsui, H. Tamamura, Y. Matsumura, and T. Yamabe, Phys. Rev. **B58,** 8163 (1998).
8. G.N. Bodarenko, V.A. Nalimova, O.V. Fateev, D. Guerard, and K.N. Semenenko, Carbon **36,** 1107 (1988).
9. V.A. Nalimova, V.V. Avdeev, and K.N. Semenenko, Mater. Sci. Forum **91–93,** 11 (1992).
10. I.T. Belash, A.D. Bronnikov, O.V. Zharikov, and A.V. Pal'nichenko, Solid State Commun. **69,** 921 (1989).
11. K. Tanaka, S. Yata, and T. Yamabe, Synth. Met. **71,** 2147 (1995).
12. S. Yata, H. Kinoshita, M. Komori, N. Ando, T. Kashiwamura, T. Harada, K. Tanaka, and T. Yamabe, Synth. Met. **62,** 153 (1994).
13. M. Endo, K. Nishimura, T. Takahashi, K. Takeuchi, and M.S. Dresselhaus, J. Phys. Chem. Solids **57,** 725 (1996). ISIC 8: Conference Proceedings, Vancouver, BC, May 1995.
14. A.W.P. Fung, Z.H. Wang, M.S. Dresselhaus, G. Dresselhaus, R.W. Pekala, and M. Endo, Phys. Rev. B **49,** 17325 (1994).
15. E. Peled, C. Menachem, D. Bar-Tow, and A. Melman, J. Electrochem. Soc. **143,** L4 (1996).
16. Y. Ein-Eli and V.R. Koch, J. Electrochem. Soc. **144,** 2968 (1997).
17. K. Nakada, M. Fujita, G. Dresselhaus, and M.S. Dresselhaus, Phys. Rev. B **54,** 17954 (1996).
18. M. Nakadaira, R. Saito, T. Kimura, G. Dresselhaus, and M.S. Dresselhaus, J. Mater. Res. **12,** 1367 (1997).
19. J.J.P. Stewart, Semi-empirical quantum chemistry library (Fujitsu Limited, Tokyo, Japan, 1993).
20. R. Saito, M. Yagi, T. Kimura, G. Dresselhaus, and M.S. Dresselhaus, J. Phys. Chem. Solids **60,** 715 (1999).